Available online at www.sciencedirect.com

SCIENCE DIRECT

Virology 339 (2005) 31 – 41

VIROLOGY

www.elsevier.com/locate/yviro

Mutational analysis of the RNA-binding domain of the Prunus necrotic ringspot virus (PNRSV) movement protein reveals its requirement for cell-to-cell movement

Ma Carmen Herranz[a], Jesús-Angel Sanchez-Navarro[a], Ana Saurí[b], Ismael Mingarro[b], Vicente Pallás[a,*]

[a]*Instituto de Biología Molecular y Celular de Plantas (IBMCP), UPV-CSIC, Avda. de los Naranjos, s/n, 46022, Valencia, Spain*
[b]*Departament de Bioquímica i Biología Molecular, Universitat de València, E-46100 Burjassot, Spain*

Received 1 March 2005; returned to author for revision 14 March 2005; accepted 11 May 2005
Available online 16 June 2005

Abstract

The movement protein (MP) of *Prunus necrotic ringspot virus* (PNRSV) is required for cell-to-cell movement. MP subcellular localization studies using a GFP fusion protein revealed highly punctate structures between neighboring cells, believed to represent plasmodesmata. Deletion of the RNA-binding domain (RBD) of PNRSV MP abolishes the cell-to-cell movement. A mutational analysis on this RBD was performed in order to identify in vivo the features that govern viral transport. Loss of positive charges prevented the cell-to-cell movement even though all mutants showed a similar accumulation level in protoplasts to those observed with the wild-type (wt) MP. Synthetic peptides representing the mutants and wild-type RBDs were used to study RNA-binding affinities by EMSA assays being approximately 20-fold lower in the mutants. Circular dichroism analyses revealed that the secondary structure of the peptides was not significantly affected by mutations. The involvement of the affinity changes between the viral RNA and the MP in the viral cell-to-cell movement is discussed.

Keywords: Prunus necrotic ringspot virus; Ilarvirus; Movement protein; RNA binding domain; Cell-to-cell movement; Subcellular location; Peptides; GFP; Circular dichroism

Introduction

Plant viruses encode the movement proteins (MPs) that play a key role in moving their genomes into neighboring cells through plasmodesmata (Carrington et al., 1996; Lazarowitz and Beachy, 1999; Waigmann et al., 2004). Based on the requirement for coat protein (CP) and on the form that the MP adopts during cell-to-cell movement, three different transport mechanisms have been reported (Callaway et al., 2001). First, viral RNA moves from cell to cell, as a ribonucleoprotein complex formed by the RNA and the MP, independently of CP, e.g., the MP of both *Tobacco mosaic virus* (TMV; Dawson et al., 1988) and *Cowpea chlorotic mottle virus* (CCMV; Rao, 1997). Second, the viral RNA is encapsidated and moved through tubular structures induced by MP, e.g., *Cowpea mosaic virus* (CPMV; Kasteel et al., 1993; van Lent et al., 1990). And third, MP requires CP but no virion formation for cell-to-cell movement, so the RNA forms a complex with both proteins, e.g., *Cucumber mosaic virus* (CMV; Blackman et al., 1998; Kaplan et al., 1998; Schmitz and Rao, 1998). In spite of the differences in the mechanism, the MPs of all the mentioned viruses belong to the '30K superfamily' (Melcher, 2000). Members of this superfamily have proved to display different functions which include: formation of tubular structures (Canto and Palukaitis, 1999; Jansen et al.,

* Corresponding author. Fax: +1 34 963877859.
E-mail address: vpallas@ibmcp.upv.es (V. Pallás).

0042-6822/$ - see front matter © 2005 Elsevier Inc. All rights reserved.
doi:10.1016/j.virol.2005.05.020

1998; Kasteel et al., 1997; Perbal et al., 1993; Zheng et al., 1997); targeting to plasmodesmata where modifies the size-exclusion limit (Ding et al., 1995; Lucas, 1995; Wolf et al., 1989); nucleic-acid binding activity (Citovsky et al., 1990; Thomas and Maule, 1995); and binding to cytoskeleton (Heinlein et al., 1995; Mc Lean et al., 1995) and microtubules (Boyko et al., 2000). Regardless of the other functions, the MPs capability of nucleic-acid binding is fundamental for virus transport. In vitro, most of these proteins preferentially bind ssRNA with no sequence specificity, and usually in a cooperative manner (Citovsky et al., 1990, 1992; Donald et al., 1997; Fujita et al., 1998; Giesman-Cookmeyer and Lommel, 1993; Herranz and Pallás, 2004; Li and Palukaitis, 1996; Schoumacher et al., 1992; Thomas and Maule, 1995; Vaquero et al., 1997). Even though the presence of a RNA-binding domain is a general feature in a large number of MPs, no relevant sequence conservation has been observed for this domain, indicating that the three-dimensional conformation could be an important requisite for their activity (Waigmann et al., 2004). In fact, two very phylogenetically distant MPs, such as TMV 30K and CarMV p7, share an inducible α-helical structure that may be important for the MP function (Brill et al., 2000; Marcos et al., 1999). Secondary structures seem to operate in the binding process in which, at least in one case, the RNA recognition appears to occur via an 'adaptative' binding mechanism wherein the RNA and the protein undergo significant conformational changes upon complex formation (Vilar et al., 2001). Although the MP requirement for the virus transport has been demonstrated in vivo through mutational analysis (Giesman-Cookmeyer and Lommel, 1993; Kim et al., 2004; Wobbe et al., 1998), there are still few studies devoted to the involvement of the RNA-binding domain of a MP in cell-to-cell movement.

Prunus necrotic ringspot virus (PNRSV) is a member of the genus Ilarvirus in the family *Bromoviridae.* The PNRSV genome consists of three plus-stranded RNAs. RNA 1 and RNA 2 encode the polymerase proteins P1 and P2; meanwhile the bicistronic RNA 3 encodes a 5′ proximal MP and the 3′ proximal CP via subgenomic RNA 4 (Aparicio et al., 2003; Sanchez-Navarro and Pallás, 1997).

Ilarvirus MPs belong to the '30K superfamily' whose members present a highly conserved domain of 30 amino acids, which may comprise a hydrophobic interaction domain (Mushegian and Koonin, 1993). Comparative sequence analyses have revealed that *Alfalfa mosaic virus* (AMV) and ilarvirus MPs have a basic region preceding the 30K motif which could function as a putative RNA binding domain (Sanchez-Navarro and Pallás, 1997). Recently, the RNA binding properties of the PNRSV MP have been demonstrated, being the first report for any member of the Ilarvirus genus. The RNA binding domain of this protein was mapped between amino acids 56–88 at the N-terminus (Herranz and Pallás, 2004). In the present study, a mutational analysis of the basic residues of the PNRSV MP RNA-binding domain was carried out, and their potential requirement for cell-to-cell movement and RNA-binding was studied both in vitro and in vivo.

Results

Subcellular localization of PNRSV MP in mesophyll and epidermal cells

The subcellular localization of PNRSV MP in mesophyll and epidermal cells was studied by agroinfiltration transient expression using the green fluorescence protein (GFP, Clontech). In addition, the transient expression of the GFP and the MP of AMV fused to the GFP were included as negative and positive controls, respectively. The fluorescence signal of the free GFP and the GFP-fused MPs was observed after 2 days post infiltration (dpi), as seen in Fig. 1. As expected, the free GFP was mainly located at the cytoplasm, and also in the nucleus in some cases (Fig. 1A). The PNRSV MP-GFP, as well as the AMV MP-GFP, were located in the cell wall of infected epidermal and mesophyll cells in punctate structures (Figs. 1B and C), indicating the resemblance between the two MPs. The GFP-MP of AMV has been reported to induce tubular structures on the periphery of infected protoplasts and in tobacco plants when expressed within the genomic RNA, although in the later case tubule formation was less abundant (Sanchez-Navarro and Bol, 2001). However, such tubular structures that either communicate cells or protrude from the cell wall were not observed by transient expression in both GFP-fused MPs, suggesting that other viral components could be required for tubule formation.

Requirement of the PNRSV MP RNA-binding domain in cell-to-cell movement

To study the potential in vivo requirement of the PNRSV MP RNA-binding domain in cell-to-cell movement, a chimeric construct of AMV RNA 3-GFP was designed (Sanchez-Navarro et al., 2001), in which the first 255 amino acids of the AMV MP were replaced by the complete MP gene of PNRSV. The resultant construct pGFP/MP-WT/CP expresses the full-length MP gene of PNRSV fused to the C-terminal 44 amino acids of the AMV MP, a hybrid protein that was previously demonstrated to be functional for the cell-to-cell transport of AMV RNA 3 (Sanchez-Navarro et al., 1997). Using the GFP reporter, the ability of the new hybrid construct to move from infected to neighboring cells in *Nicotiana tabaccum* plants that constitutively express the P1 and P2 polymerase proteins of AMV (P12 plants; Van Dun et al., 1988) was analyzed. P12 leaves and protoplasts were inoculated with transcripts of the construct carrying the full-length MP gene of PNRSV and the fluorescent signals monitored by a confocal laser scanning microscope (CLSV) (Fig. 2A). Single fluorescent cells at 2 dpi were observed to become clear foci at 4 dpi. The fluorescent signal was

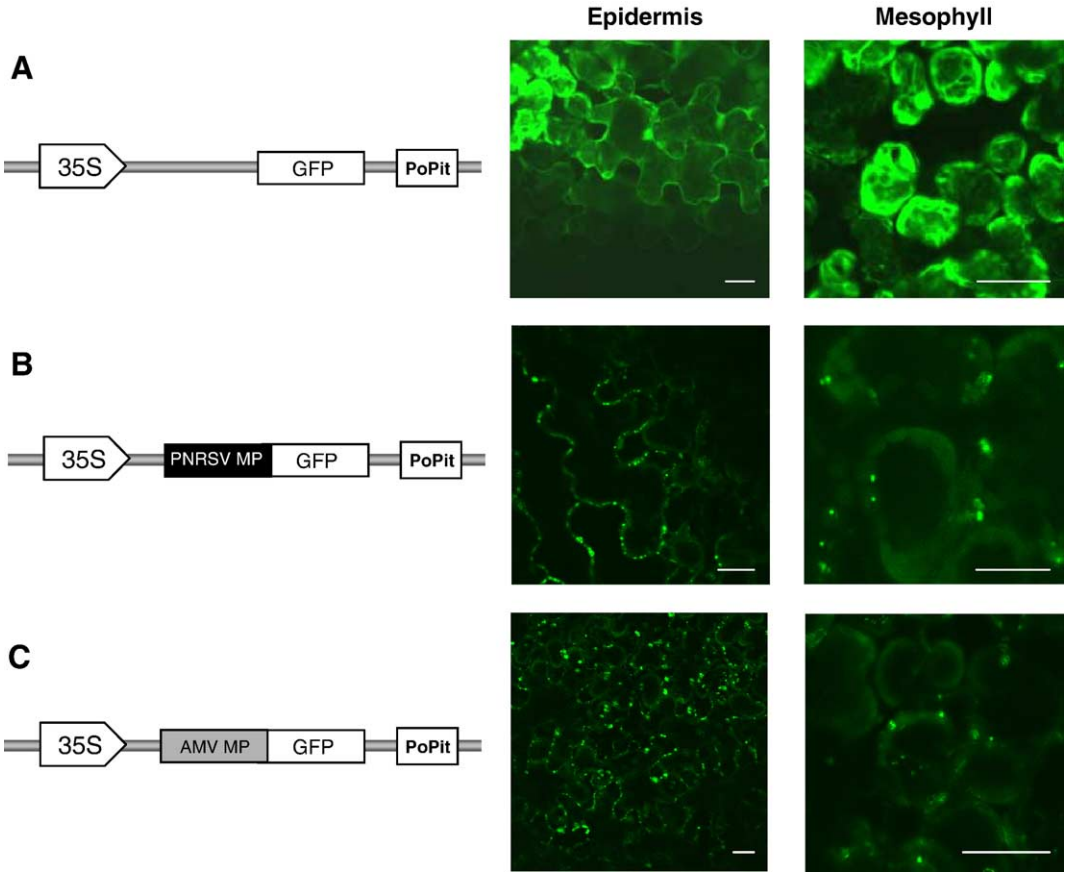

Fig. 1. Detection of green fluorescence in *Nicotiana tabacum* plants after agroinfiltration with the GFP (A); the GFP fused to the PNRSV MP (B) and AMV MP (C), under the control of the 35S promoter from *cauliflower mosaic virus* (CaMV) and the *potato proteinase inhibitor terminator* (PoPit). Fluorescence was monitored 2 days after infiltration with a confocal laser scanning microscope.

detected on P12 protoplasts after 18 h post transfection. These results demonstrate that the chimeric construct is functionally active in facilitating the intercellular transport of a chimeric AMV RNA 3.

The RNA-binding domain (RBD) of the PNRSV MP has been recently mapped in vitro between amino acids 56–88 (Herranz and Pallás, 2004). This motif was firstly deleted in construct pGFP/MP-ΔRBD/CP (Fig. 2B) to analyze in vivo the role of the RBD of the PNRSV MP. This MP region contains 9 basic residues that could potentially be directly involved in RNA binding, and could thus modulate the virus transport. Then, a mutational analysis was carried out in which the nine basic amino acids were changed into groups of three by non-charged alanine or glycine residues (see Figs. 2C–E). The secondary structure of the resulting mutated MPs analyzed by different secondary structure prediction algorithms did not show any significant alteration. Transcripts derived from all constructs were inoculated in P12 plants, and the results were summarized in Fig. 2. As this figure shows, the RBD deletion rendered a hybrid virus unable to move from cell to cell, showing single infected cells at 2 dpi. However, no infection foci were observed at 4 dpi (Fig. 2B). Similar results were observed with mutants where basic amino acids within the RBD were replaced by non-charged ones (Figs. 2C–E). Apparently, the absence of three positive charges, independently of their position within the RBD, is sufficient to block the virus transport. Such virus transport blockage was not observed when three basic amino acids (K196, K199 and K204) outside the RBD were changed to non-charged alanine residues (Fig. 2G), indicating that the presence of positively charged residues within the RBD is critical for virus transport.

The three N-terminal basic residues of the RBD were conservatively replaced by the corresponding positively charged amino acids to analyze the importance of the specific basic amino acids located at this region (pGFP/MP-K57R.R62K.K66R/CP; Fig. 2F). The resultant construct showed similar infection foci than the wild-type hybrid virus, indicating that the presence of positive charges (and not their sequence specificity) is a major determinant for virus transport.

The different MP constructs were then assayed in P12 protoplasts, and the viral RNA accumulation levels were analyzed by Northern blot. All the AMV RNA 3 derivatives showed clear fluorescent cells (Figs. 2A–G, protoplasts)

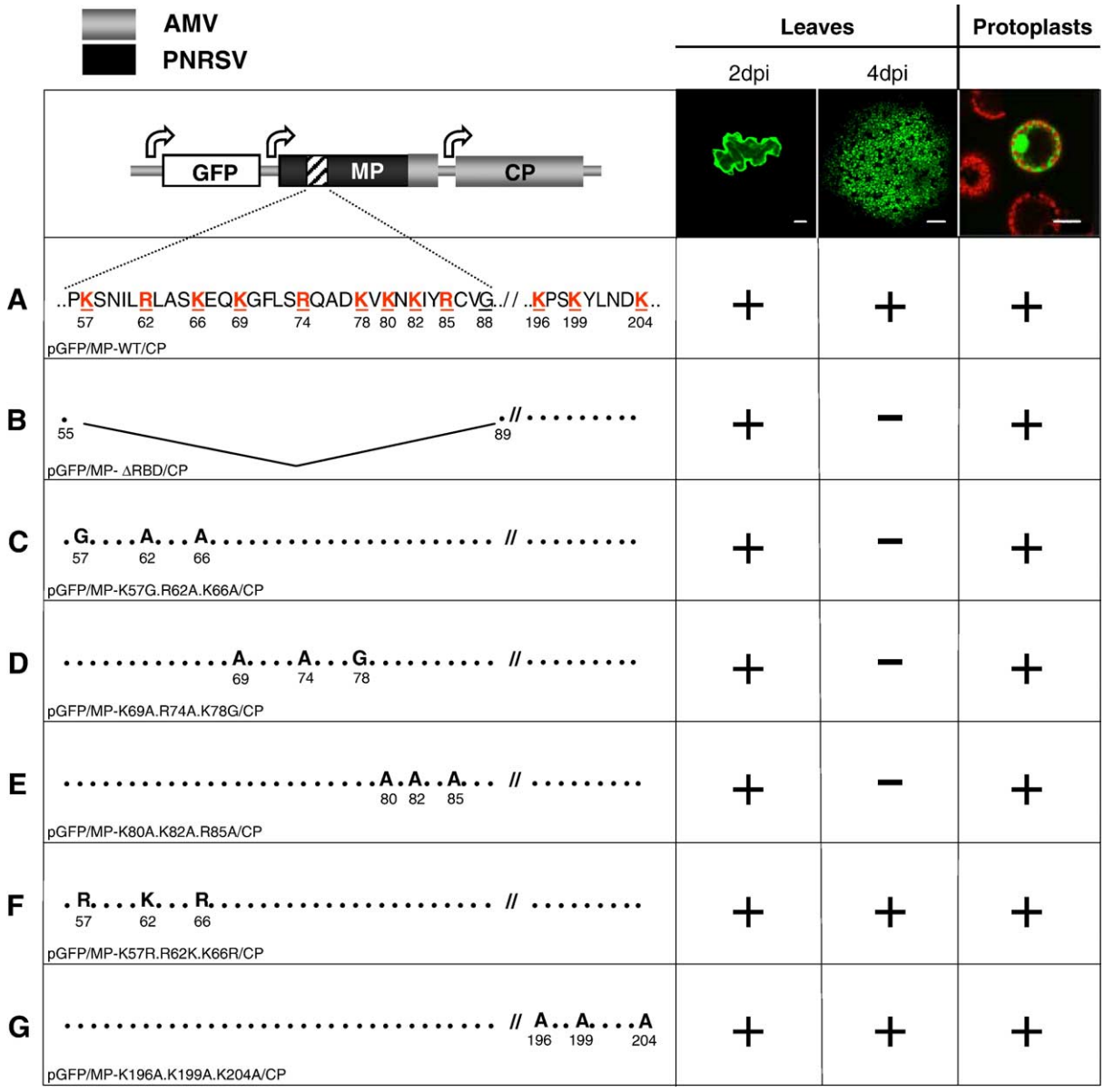

Fig. 2. Detection of green fluorescence in P12 plants and protoplasts inoculated with transcripts carrying different PNRSV movement protein (MP) mutants. P12 plants and protoplasts were inoculated with RNA 3 transcripts from plasmids: pGFP/MP-WT/CP (A), pGFP/MP-ΔRBD/CP (B), pGFP/MP-K57G.R62A.K66A/CP (C), pGFP/MP-K69A.R74A.K78G/CP (D), pGFP/MP-K80A.K82A.R85A/CP (E), pGFP/MP-K57R.R62K.K66R/CP (F) and pGFP/MP-K196A.K199A.K204A/CP (G). Schematic representation of the pGFP/MP-WT/CP construct is shown on the top left. Sequences derivate from *Alfalfa mosaic virus* (AMV) or *Prunus necrotic ringspot virus* (PNRSV) are represented in grey and black colors, respectively. The RNA binding domain of the MP of PNRSV is indicated as a lined box and the amino acid sequence is presented in panel (A). Numbers indicate the corresponding amino acid of the MP of PNRSV. The new residue introduced in each construct is indicated with the corresponding letter meanwhile the no changed amino acids are indicated as a dot. Fluorescence was monitored 2 and 4 days post inoculation (dpi) in P12 plants or 18 post transfection hours in protoplasts, using a confocal laser scanning microscope and an excitation at 488 nm and an emission at 500–535 nm. In protoplasts, the chloroplasts were visualized by excitation at 543 nm and emission at 555–700 nm. Bar represent 20 μm (leaves at 2 dpi and protoplasts) or 200 μm (leaves at 4 dpi).

indicating their ability to replicate and express the GFP reporter gen. In addition, all constructs accumulated similar levels of viral RNAs (Fig. 3A lanes 1–7) to the progeny when compared with the AMV RNA 3 wild-type (Fig. 3A lane 9). In accordance with the similar viral RNA 4 accumulation levels observed, Western blot analysis performed with an antiserum against the CP showed that all constructs rendered similar protein levels (Fig. 3B). Apparently, the different modifications introduced in the MP of PNRSV were not affecting the replication and expression processes of the chimeric viruses. Thus, the inability of these chimeras to move from cell to cell cannot be attributed to differences in their replication/accumulation level.

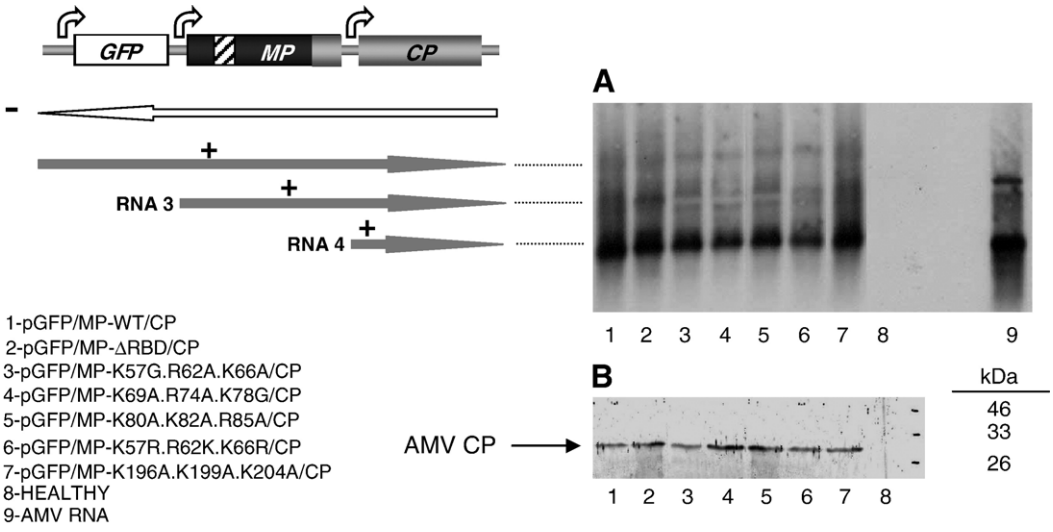

Fig. 3. Northern and Western blots analyses of the accumulation of *Alfalfa mosaic virus* (AMV) quimeras in P12 protoplasts. (A) Northern blot analysis of the accumulation of RNAs 3 and 4 in P12 protoplasts inoculated with chimeric AMV-PNRSV transcripts. Glyoxylated RNAs extracted from inoculated P12 protoplasts were loaded on 1% agarose gels, and hybridized with a dig-riboprobe complementary to the AMV 3′NTR. Protoplasts were inoculated with RNA 3 transcripts from plasmids; pGFP/MP-WT/CP (lane 1), pGFP/MP-ΔRBD/CP (lane 2), pGFP/MP-K57G.R62A.K66A/CP (lane 3), pGFP/MP-K69A.R74A.K78G/CP (lane 4), pGFP/MP-K80A.K82A.R85A/CP (lane 5), 6-pGFP/MP-K57R.R62K.K66R/CP (lane 6), pGFP/MP-K196A.K199A.K204A/CP (lane 7), healthy (lane 8), and AMV RNA (lane 9). The positions of plus-strand AMV RNA 3 and 4 are indicated in the left margin. (B) Western blot analysis of accumulation of the AMV CP in P12 protoplasts inoculated with chimeric AMV-PNRSV transcripts.

RNA binding properties

Recombinant viral MPs typically form insoluble inclusion bodies, which are difficult to manipulate for biochemical and biophysical characterization. In order to perform RNA binding studies, it has been previously shown that peptides harboring independent RNA-binding domains can mimic the binding properties of the intact proteins (e.g., Ansel-McKinney et al., 1996; Aparicio et al., 2003; Marcos et al., 1999; Tan and Frankel, 1995; Vilar et al., 2001). To explore the RNA-binding abilities of the RBD mutants studied in vivo, four peptides containing the central region of this domain were synthesized (Fig. 4, top): a peptide containing the wild-type sequence and three peptides corresponding to the mutants that were unable to move from cell to cell (Figs. 2C–E). The binding of the peptides to the PNRSV RNA 4 was assayed by EMSA (Carey, 1991). A constant amount of [α-^{32}P]UTP-labeled RNA transcript (PNRSV RNA 4) was incubated with increasing amounts of each peptide (0.5–100 μM). The assayed peptides maintained the RNA-binding capability as shown in Fig. 4, although differences in the affinity were significant. The disappearance of the free RNA was quantified by film densitometry to calculate the apparent K_d of each peptide–RNA interaction. Data from at least two independent experiments were used to generate a linear regression curve, from which the peptide concentration at which half of the RNA bound, was estimated to be: 0.9 μM for the wild-type peptide; 23.6 μM for the RBD-R62A/K66A, 18.6 μM for the RBD-K69A/R74A/K78G, and 25.0 μM for the RBD-K80A/K82A/R85A. The affinities of the three substitution peptides for the RNA were around 20-fold lower than that of the wild-type peptide, and no significant differences were observed among them. Interestingly, there is a good correlation in the RNA binding capacity between the wild type peptide (K_d = 0.9 μM) and the full-length protein (K_d = 1.4 μM) (Herranz and Pallás, 2004), suggesting that the present results using peptides reflect the binding behavior of the correspondent mutant proteins.

Circular dichroism (CD) spectroscopy

To better understand the RNA binding capacity observed for the different peptides, a structural characterization of these peptides using CD spectroscopy was performed. This technique allows a qualitative analysis of the content in secondary structure of the peptides, and was used to discern whether the differences in the RNA-binding capacity between the wild-type and the mutant sequences arise from the loss of positively-charged residues or from differences in the structure of this region induced by the substitutions. All four peptides are highly flexible without a discernible secondary structure in aqueous solution, in a good agreement with what has been previously found with similar RBD-derived peptides from MPs (Vilar et al., 2001, in press). Nevertheless, propensity to fold into a α-helix in the presence of different secondary structure inducers (like TFE and SDS) correlated with the RNA-binding capacity of the peptides observed in the EMSA experiments (Fig. 4). It has to be noted that all four peptides retain the RNA binding capacity and that nascent secondary structure elements would be necessary to facilitate the appropriate interface

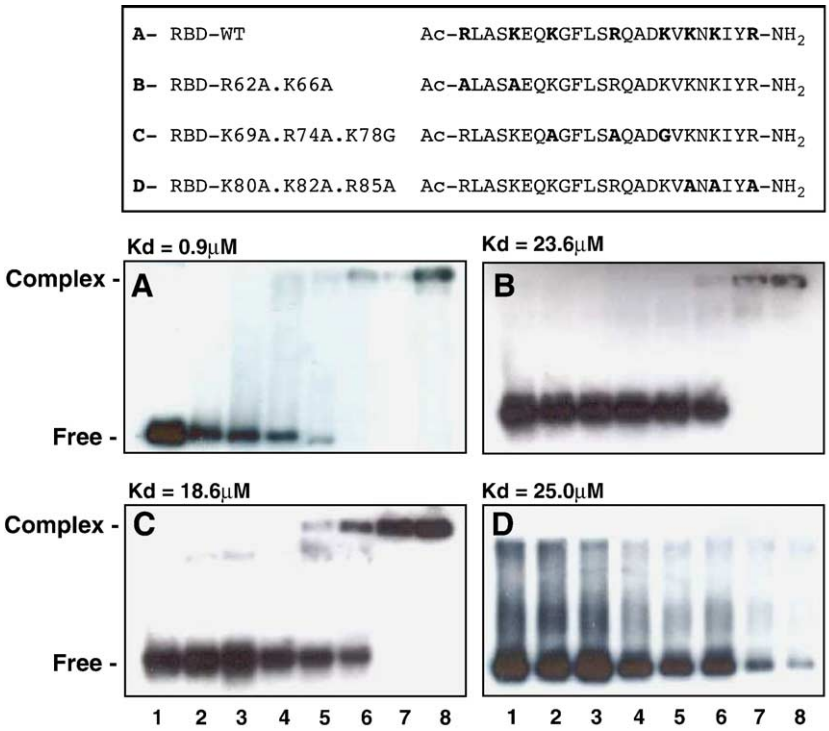

Fig. 4. RNA-binding analysis of the RBD-derived peptides by EMSA. 5 ng of [α-^{32}P]UTP-PNRSV-RNA 4 transcript was incubated with no peptide (lane 1), or with increasing concentrations of each synthetic peptide; 0.5 μM (lane 2), 1 μM (lane 3), 2 μM (lane 4), 5 μM (lane 5), 10 μM (lane 6), 50 μM (lane 7), and 100 μM (lane 8), subjected to electrophoresis, transferred to positively-charged nylon membranes, fixed to the membranes with a UV cross-linker (700 × 100 μJ/cm^2) and exposed to X-ray film. Peptide sequences of the wild type (A) or mutated RNA binding domains (B, C and D) are shown at the top. Exchanged amino acids are indicated by the corresponding letter meanwhile the unmodified ones are represented by dots. The position of the 'complex' and 'free' RNA is indicated on the left.

between each RBD-derived peptide and the viral RNA. As an example, Fig. 5 shows the CD spectra of the peptides in buffer solution and also in the presence of increasing trifluoroethanol (TFE) concentrations (20, 40, 60, and 70%). As inferred form these data and from the data derived from the SDS spectra (Table 1), a conformational transition towards stabilization of α-helical structures were observed in all of the far UV CD spectra upon addition of inducers even at low concentrations, and with no significant differences between the wild-type and the mutant peptides. Thus, the positive charges replaced in each mutant were not affecting its secondary structure, even though they were still responsible for the differences in the RNA-binding activity.

Discussion

MPs are encoded by most plant viruses for the translocation of the viral progeny between cells. Despite the vast diversity of MPs (Melcher, 2000), RNA binding activity has been demonstrated for a large number of them (Waigmann et al., 2004), suggesting that this function must be bio-

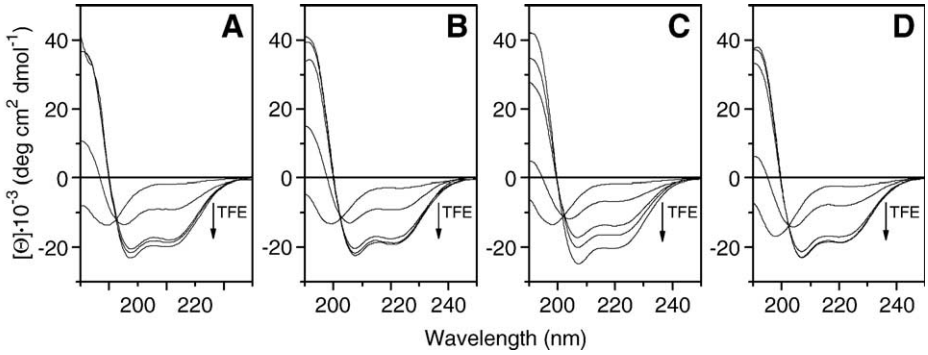

Fig. 5. Far UV CD spectra of RBD-derived peptides. The four peptides (sequences shown in Fig. 4) were analyzed in the presence of increasing concentrations of a secondary structure inductor, TFE (20, 40, 60, and 70%, as the arrow indicates). Peptide concentration was 30 μM in 5 mM MOPS/NaOH buffer, pH 7.0 at 25 °C. (A) RBD-WT; (B) RBD-R62A.K66A; (C) RBD-K69A.R74A.K78G; (D) RBD-K80A.K82A.R85A.

Table 1
Secondary structure (%) of the RBD-derived peptides after analysis of the CD spectra using the CDPro package

Peptide[a]	Medium	H[b]	S[c]	t[d]	r[e]
A	Buffer[f]	4	33	23	40
	5 mM SDS	42	10	20	28
	40% TFE	56	7	17	20
B	Buffer	5	20	12	63
	5 mM SDS	43	10	18	29
	40% TFE	50	11	16	23
C	Buffer	2	24	14	60
	5 mM SDS	37	13	20	30
	40% TFE	45	9	17	29
D	Buffer	4	14	10	72
	5 mM SDS	50	6	14	30
	40% TFE	55	4	13	28

[a] Peptide sequences are shown in Fig. 4.
[b] H: accumulated value for regular and distorted α-helix.
[c] S: accumulated value for regular and distorted β-strand.
[d] t: turn.
[e] r: random.
[f] Buffer medium was 10 mM Tris–HCl pH 7.5.

logically important in the viral life cycle. However, the in vivo significance is poorly understood except for a few cases. PNRSV belongs to the family *Bromoviridae* for which four different RBDs have been mapped (Fujita et al., 1998; Herranz and Pallás, 2004; Schoumacher et al., 1994; Vaquero et al., 1997). Although no significant sequence similarity was observed, all of them share a high proportion of basic amino acids.

PNRSV MP behaves as a true MP since its transient expression, when fused to the GFP reporter, revealed highly fluorescent punctate structures between neighboring cells (Fig. 1). A similar subcellular location was observed using the AMV MP-GFP (Fig. 1C) for which its accumulation in structurally modified plasmodesmata has been previously reported (van der Wel et al., 1998). The absence of other viral components during transient expression indicates that the PNRSV MP contains all determinants to be targeted to the periphery of the cell, as previously reported for the AMV MP on protoplasts (Zheng et al., 1997). However, no tubular structures protruding from the cell periphery (or crossing between) were observed suggesting that, as in the case of AMV, other viral components are required for such structures (Sanchez-Navarro and Bol, 2001). The AMV and PNRSV MPs are closed phylogenetically related, and the similar subcellular location reported here is consistent with the observation that an AMV RNA3 bearing the PNRSV MP is competent for cell-to-cell movement in *Nicotiana tabaccum* plants, a non-permissible host for PNRSV (Sanchez-Navarro et al., 1997).

The PNRSV MP RBD was recently mapped between amino acids 56 and 88 (Herranz and Pallás, 2004) being the smallest domain characterized in the *Bromoviridae* family. RBD deletion from the PNRSV MP rendered a protein that was unable to interact with RNA in vitro (Herranz and Pallás, 2004). When the mutated PNRSV MP gene, lacking the RBD, replaced the MP gene of an AMV RNA3, the hybrid virus was unable to move from cell to cell, thus suggesting that RNA-binding is a critical activity for virus transport. A similar situation has been observed in a CMV MP when part of the RNA-binding domain was deleted (Vaquero et al., 1997). In addition, the RNA-binding activity of the N-terminal extension domain of *Poa semilatent virus* 63 kDa protein has been associated to the long distance virus movement (Kalinina et al., 2001). An alanine scanning mutagenesis of amino acid residues of the RBD of the BMV MP showed their importance for cell-to-cell movement (Takeda et al., 2004).

To further analyze the role of the RBD in virus transport in vivo, we performed point mutations of nine positively charge residues present in this region. Exchange of the different basic residues (in boxes of three residues) of the RBD of the MP of PNRSV by the non-charged alanine or glycine amino acids rendered an MP unable to allow the cell-to-cell movement of the AMV hybrid constructs (Figs. 2C, D and E), indicating their critical role in the MP activity. Interestingly, functional mutant MPs were obtained by conservative replacement of positively-charged residues (Fig. 2F), and when mutations (basic residues exchanged by non-charged residues) were performed outside the RBD (Fig. 2G), suggesting that the presence of positive charges within the RBD, and not their specific sequence, are critical for MP activity, probably due to their role in RNA interaction. In this sense, the cell-to-cell movement of mutant BMV MPs in which at least one positively-charged residue of the RBD was exchanged by alanine is also affected, while the majority of the positive residues exchanged outside the RBD rendered functional MPs (Takeda et al., 2004).

All mutants presented a similar accumulation level in protoplast to those observed for the wild-type (Fig. 2). This result, together with the previous observation that some AMV mutants that accumulated the 5% level of the wild type in protoplasts were able to induce infection foci of wild type size (Sanchez-Navarro and Bol, 2001; Tenllado and Bol, 2000) strongly suggests that differences in affinity to RNA, and not to the replication level, are responsible for the marked differences found in cell-to-cell transport. Synthetic peptides representing these mutants and the wild-type sequence were used in EMSA assays to demonstrate this hypothesis. The observation that the dissociation constant (K_d) obtained with the synthetic peptide that comprises the RBD wild-type (0.9 μM) was comparable to that obtained with the full-length MP in vitro (1.4 μM; Herranz and Pallás, 2004) validates the use of the present approach. Interestingly, the three RBD mutants that were unable to move in vivo, bound the RNA with an affinity approximately 20-fold lower than the wild-type (18.6–25 μM versus 0.9 μM), and no significant differences were observed among their constant values, thus suggesting a similar contribution of all basic residues present along the domain. In addition, the secondary structure analysis of the

different synthetic peptides by CD spectroscopy showed that the ability to fold into an α-helix present in the wild-type domain was maintained in the three mutant RBD-derived peptides, indicating that the decrease of their binding affinities was not related with significant changes in the secondary structure of the peptides, rather it was related with the loss of potential interactions with the RNA. All in all, we have established a correlation between the movement phenotype in vivo and the binding and structural properties of RBD-derived peptides in vitro.

Our results clearly demonstrated that significant changes in the RNA-binding capacity of a MP RBD have dramatic biological consequences on the life viral cycle. MP–RNA interactions must be compatible with other viral processes (e.g., replication, expression or even encapsidation). Thus, a MP with an excessively high RNA affinity could block part of the viral process (e.g., impeding the entry of the ribosomes or the replicase complexes). Meanwhile, a MP with an excessively low RNA affinity could be insufficient to translocate the viral progeny to the adjacent healthy cells. It has been previously shown that an amino acid change in the RBD of TCV MP alters both the RNA-binding capability of the protein as well as the systemic spread of the virus (Wobbe et al., 1998), although unfortunately, the affinity differences were not quantified. On the other hand, Giesman-Cookmeyer and Lommel (1993) and Kim et al. (2004) have shown that mutants at 20% of the RNA-binding capability (in other words, with 5-fold lower affinity) are functional in cell-to-cell movement, although their systemic movement may be impeded. Thus, it is tempting to speculate that variations of the RNA-binding affinity of MPs are permissible up to a limited range (5-fold or less), whereas more significant deviations of the theoretical K_d would not be compatible with their biological function.

Materials and methods

Constructions of AMV and PNRSV MPs fused to GFP clones

The PNRSV MP was amplified by PCR using the VP360 sense primer (5′-GCATCCATGGCCGGTGTCAGTAA-AAAC-3′ containing a *Nco*I site, underlined) and the VP361 antisense primer (5′-CGATGCTAGCAATTCCA-GAACT-3′ with a *Nhe*I site, underlined). The *Nco*I–*Nhe*I fragment was fused to the 5-termini of the GFP using the pUC 21 vector. The fused genes PNRSV MP:GFP and AMV MP:GFP (extracted from construct pMP:GFP/MP/CP, Sanchez-Navarro and Bol, 2001) were then subcloned into the pIC843P vector, between the 35S promoter from *cauliflower mosaic virus* (CaMV) and the *potato proteinase inhibitor terminator* (PoPit), using the *Nco*I–*Pst*I restriction enzymes. Finally, the resultant 35S-MP:GFP-PoPit cassettes were introduced into the *Xho*I digested pMOG800 binary vector.

Agroinfiltration

Binary pMOG800 plasmids carrying the 35S-AMV MP:GFP-PoPit or 35S-PNRSV MP:GFP-PoPit cassettes were transformed into *A. tumefaciens* strain C58C1, containing the virulence helper plasmid pCH32. *Agrobacterium* cells were inoculated into 5 ml L-broth medium supplemented with kanamycin, tetracycline and rifampicine at a final concentration of 50 μg/ml and incubated at 28 °C for 2 days. The cultures were then pelleted and resuspended in a solution containing 10 mM $MgCl_2$, 10 mM MES pH 5.6 and 150 μM acetosyringone to a final concentration of 0.5 DO_{600}. Cultures were incubated at room temperature for 2 h before agroinfiltration. Agroinfiltration was carried out as previously described (Vlot et al., 2001).

Construction of chimeric GFP-AMV cDNA 3 clones

Wild-type and truncated PNRSV MP cDNAs were amplified by PCR from the plasmids pMAL200/104 and pMAL200Δ104, respectively (Herranz and Pallás, 2004) using the previously described VP360/VP361 primers. The *Nco*I–*Nhe*I PCR fragments were exchanged with the *Nco*I–*Nhe*I fragment of plasmid pGFP/A255/CP (Sanchez-Navarro and Bol, 2001). Constructs carrying single amino acid mutations within or outside of the RNA binding domain were obtained after three PCRs. Overlapping N-terminal and C-terminal regions of each MP mutant were amplified in two different PCR reactions using the specific primers containing the corresponding mutation (see Table 2). The gel-extracted PCR products were then mixed and used as a template in a third PCR reaction, using the primers VP360 and VP361 to amplify the complete MP gene. The final PCR products were digested with *Nco*I–*Nhe*I and exchanged with the *Nco*I–*Nhe*I fragment of the plasmid pGFP/A255/CP, which resulted in the different constructs listed in Fig. 2.

Inoculation of P12 protoplast and plants

Plasmids containing either the wild-type or the different mutants of the PNRSV MP were linearized with *Pst*I and transcribed with T7 RNA polymerase. Protoplasts were extracted from P12 transgenic *Nicotiana tabaccum* plants and 2.5×10^5 protoplasts were inoculated by the polyethylene glycol method (Loesch-Fries et al., 1985) with 6 μl of the transcription mixture. P12 plants were grown and inoculated with RNA transcripts, as previously described (Taschner et al., 1991). The GFP expression in protoplast and plants was analyzed with a Leica TCS SL confocal laser scanning microscope (Leica), with excitation at 488 nm and emission at 500–535 nm.

Northern blot assays

Total RNA was extracted from protoplasts at 18 h post inoculation using TRI Reagent (Sigma Steinheim, Ger-

Table 2
Primers used to amplify the different PNRSV MP mutants

pGFP/MP-WT/CP	s	VP360	5′-GCATCCATGGCCGGTGTCAGTAAAAAC-3′	*Nco*I
	as	VP361	5′-CGATGCTAGCACTTCCAGAACT-3′	*Nhe*I
pGFP/MP-ΔRBD/CP	s	VP360	5′-GCATCCATGGCCGGTGTCAGTAAAAAC-3′	*Nco*I
	as	VP361	5′-CGATGCTAGCACTTCCAGAACT-3′	*Nhe*I
pGFP/MP-K57G.R62A.K66A/CP	N-t^{s}	VP360	5′-GCATCCATGGCCGGTGTCAGTAAAAAC-3′	*Nco*I
	N-t^{as}	VP464	5′-TGCCAGTATATTGGATCCCGGGAGGTTAACC-3′	
	C-t^{s}	VP463	5′-**GGA**TCCAATATACTG**GCA**TTAGCGAGT**GCG**GAGCAGAAAGGT-3′	
	C-t^{as}	VP361	5′-CGATGCTAGCACTTCCAGAACT-3′	*Nhe*I
pGFP/MP-K69A.R74A.K78G/CP	N-t^{s}	VP360	5′-GCATCCATGGCCGGTGTCAGTAAAAAC-3′	*Nco*I
	N-t^{as}	VP466	5′-GGCCGAGAGGAAACCTGACTGCTCCTTACT-3′	
	C-t^{s}	VP465	5′-**GCA**GGTTTCCTCTCG**GCC**CAGGCCGAT**GGA**GTAAAGAATAAA-3′	
	C-t^{as}	VP361	5′-CGATGCTAGCACTTCCAGAACT-3′	*Nhe*I
pGFP/MP-K80A.K82A.R85A/CP	N-t^{s}	VP360	5′-GCATCCATGGCCGGTGTCAGTAAAAAC-3′	*Nco*I
	N-t^{as}	VP467	5′-GCCTACGCATGCGTAAATTGCATTCGCTACTTTATCGGCCTG-3′	
	C-t^{s}	VP468	5′-**GCG**AAT**GCA**ATTTAC**GCA**TGCGTAGGCCGAGTATTC-3′	
	C-t^{as}	VP361	5′-CGATGCTAGCACTTCCAGAACT-3′	*Nhe*I
pGFP/MP-K57R.R62K.K66R/CP	N-t^{s}	VP360	5′-GCATCCATGGCCGGTGTCAGTAAAAAC-3′	*Nco*I
	N-t^{as}	VP506	5′-TTTCAGTATATTGGATCTCGGGAGGTTAACC-3′	
	C-t^{s}	VP505	5′-**AGA**TCCAATATACTG**AAA**TTAGCGAGTAG**AGA**GCAGAAAGGT-3′	
	C-t^{as}	VP361	5′-CGATGCTAGCACTTCCAGAACT-3′	*Nhe*I
pGFP/MP-K196A.K199A.K204A/CP	N-t^{s}	VP360	5′-GCATCCATGGCCGGTGTCAGTAAAAAC-3′	*Nco*I
	N-t^{as}	VP568	5′-CGCATCATTAAGATATGCCGAAGGTGCTGT-3′	
	C-t^{s}	VP567	5′-ACA**GCA**CCTTCG**GCA**TATCTTAATGAT**GCG**-3′	
	C-t^{as}	VP361	5′-CGATGCTAGCACTTCCAGAACT-3′	*Nhe*I

s: sense primer; a: antisense primer. Engineered restriction sites are underlined. Nucleotides in bold represent the different mutations.

many). The RNAs were electrophoresed through formaldehyde-denatured gel and transferred to positively charged nylon membranes (Roche Mannheim, Germany). RNAs were fixed to the membranes with a UV cross-linker (700×100 μJ/cm^2). Hybridization and detection was conducted as previously described (Pallás et al., 1998) using a dig-riboprobe (Roche Mannheim, Germany) complementary to the AMV 3′UTR.

Western blot assays

Total proteins extracted from protoplasts at 18 h post inoculation were electrophoresed through 12% SDS-polyacrylamide gels and transferred to nitrocellulose membranes (Bio-Rad). Proteins were probed with the antiserum raised against AMV-CP diluted 1:2000. Antibody binding was detected by immunoreaction to anti-rabbit IgG couple to alkaline phosphatase, and subsequent colorimetric detection was performed using NBT-BCIP substrate as described (Gómez and Pallás, 2004).

Synthesis of the RBD-derived peptides

Peptides were synthesized as acetylated N-terminal and C-terminal amides using standard Fmoc chemistry on a 433A peptide synthesizer (Applied Biosystems), and purified by HPLC. Matrix-assisted laser desorption ionization-time-of-flight mass spectrometry was used to confirm peptide identity. Peptide concentrations were determined by UV spectroscopy for RNA-binding assays and spectroscopy studies, using $\varepsilon_{276} = 1450\ M^{-1}\ cm^{-1}$ for tyrosine.

Circular dichroism

All measurements were carried out on a Jasco J-810 CD spectropolarimeter, in conjunction with a Neslab RTE 110 waterbath and temperature controller. CD spectra were the average of a series of ten scans taken at 0.2 nm intervals. CD spectra of the same buffer (or in the presence of trifluoroethanol (TFE) as described in the figure legends) without peptide were used as baseline in all the experiments. The peptide concentration was 30 μM in all cases. Data analysis was performed in all cases with the help of the CDPro software package, which contains three commonly used programs: SELCON3, CONTIN/LL and CDSSTR (Sreerama and Woody, 2000). This software allows the use of different reference sets of proteins, including non-structured proteins, to increase the reliability of the analysis with our peptides since they are not folded in plain buffered solutions.

Eletrophoretic mobility shift assays (EMSA)

Plasmid containing a full-length cDNA copy of RNA 4 of PNRSV (Sanchez-Navarro and Pallás, 1994) was digested with *Sac*I and labeled with [α-^{32}P] UTP in a *in vitro* transcription reaction using T3 RNA polymerase. The resulting transcript was purified over a Sephadex G-50 (Pharmacia) column. For the EMSA, 5 ng of transcript and protein concentrations of 0.5 to 100 μM of each peptide in a total volume of 10 μl were used in a binding reaction. Reaction mixtures were incubated for 30 min at room temperature in binding buffer (BB; 10 mM Tris–HCl, pH

8.0, 100 mM NaCl, 50% glycerol, 2U HPRI RNase inhibitor) as described previously (Gómez et al., 2005).

After the incubations, 2 μl of tracking dye was added and the samples were separated by electrophoresis through a 1% agarose gel at 80 V in TAE (40 mM Tris–acetate, 1 mM EDTA, pH 8.0). RNAs were transferred to positively-charged nylon membranes (Roche Diagnostics) by capillarity in TAE overnight. RNAs were fixed to the membranes with a UV cross-linker (700×100 μJ/cm^2) and exposed to X-ray film.

Acknowledgments

This work was supported by Grant BIO02-04099 from the Spanish granting agency DGICYT. J.A.S-N was the recipient of a contract from the Ramón y Cajal program of the Ministerio de Educación y Ciencia of Spain. MC.H. and A.S. were recipients of a fellowship from the Ministerio de Educación y Ciencia of Spain.

References

Aparicio, F., Vilar, M., Perez-Paya, E., Pallás, V., 2003. The coat protein of prunus necrotic ringspot virus specifically binds to and regulates the conformation of its genomic RNA. Virology 15 (313), 213–223.

Ansel-McKinney, P., Scott, S.W., Swanson, M., Ge, X., Gehrke, L., 1996. A plant viral coat protein RNA binding consensus sequence contains a crucial arginine. EMBO J. 15 (24), 7188–7189.

Blackman, L.M., Boevink, P., Santa Cruz, S., Palukaitis, P., Oparka, K.J., 1998. The movement protein of cucumber mosaic virus traffics into sieves elements in minor veins of *Nicotiana clevelandii*. Plant Cell 10 (4), 525–537.

Boyko, V., Ferralli, J., Ashby, J., Schellenbaum, P., Heinlein, M., 2000. Function of microtubules in intercellular transport of plant virus RNA. Nat. Cell Biol. 2 (11), 826–832.

Brill, L.M., Nunn, R.S., Kahn, T.W., Yeager, M., Beachy, R.N., 2000. Recombinant tobacco mosaic virus movement protein is an RNA-binding, alpha-helical membrane protein. Proc. Natl. Sci. U.S.A. 97 (13), 7112–7117.

Callaway, A., Giesman-Cookmeyer, D., Gillock, E.T., Sit, T.L., Lommel, S.A., 2001. The multifunctional capsid proteins of plant RNA virus. Annu. Rev. Phytopathol. 39, 419–460.

Canto, T., Palukaitis, P., 1999. Are tubules generated by the 3a protein necessary for cucumber mosaic virus movement? Mol. Plant-Microb. Interact. 12 (8), 985–993.

Carey, J., 1991. Gel retardation. In: Sauer, R.T. (Ed.), Methods in Enzymology. Protein–DNA Interactions. Academic Press, San Diego, CA, pp. 103–117.

Carrington, J.C., Kasschau, K.D., Mahajan, S.K., Schaad, M.C., 1996. Cell-to-cell and long-distance transport of viruses in plants. Plant Cell 8 (10), 1669–1681.

Citovsky, V., Knorr, D., Schuster, G., Zambryski, P., 1990. The P30 movement protein of tobacco mosaic virus is a single-strand nucleic acid binding protein. Cell 60 (4), 637–642.

Citovsky, V., Wong, M.L., Shaw, A.L., Venkataram, P.B.V., Zambryski, P., 1992. Visualisation and characterisation of tobacco mosaic virus movement protein binding to single-stranded nucleic acids. Plant Cell 4 (4), 397–411.

Dawson, W.O., Bubrick, P., Grantham, G.L., 1988. Modifications of the tobacco mosaic virus coat protein gene affecting replication, movement, and symptomatology. Phytopathology 78 (6), 783–789.

Ding, B.A., Li, Q.B., Nguyen, L., Palukaitis, P., Lucas, W.J., 1995. Cucumber mosaic virus 3a protein potentiates cell-to-cell trafficking of CMV RNA in tobacco plants. Virology 207 (2), 345–353.

Donald, R.G., Lawrence, D.M., Jackson, A.O., 1997. The barley stripe mosaic virus 58-kilodalton beta(b) protein is a multifunctional RNA binding protein. J. Virol. 71 (2), 1538–1546.

Fujita, M., Mise, K., Kajiura, Y., Dohi, K., Furusawa, I., 1998. Nucleic acid-binding properties and subcellular localisation of the 3a protein of brome mosaic bromovirus. J. Gen. Virol. 79 (5), 1273–1280.

Giesman-Cookmeyer, D., Lommel, S.A., 1993. Alanine scanning mutagenesis of a plant virus movement protein identifies three functional domains. Plant Cell. 5 (8), 973–982.

Gómez, G., Pallás, V., 2004. A long-distance translocatable phloem protein from cucumber forms a ribonucleoprotein complex in vivo with Hop stunt viroid RNA. J. Virol. 78 (18), 10104–10110.

Gómez, G., Torres, H., Pallás, V., 2005. Identification of translocatable RNA-binding phloem proteins from melon, potential components of the long-distance RNA transport system. Plant J. 41, 107–116.

Heinlein, M., Epel, B.L., Padgett, H.S., Beachy, R.N., 1995. Interaction of tobamovirus movement proteins with the plant cytoskeleton. Science 270 (5244), 1983–1985.

Herranz, M.C., Pallás, V., 2004. RNA-binding properties and mapping of the RNA-binding domain from the movement protein of Prunus necrotic ringspot virus. J. Gen.Virol. 85 (3), 761–768.

Jansen, K.A.J., Wolfs, J.A.M., Lohuis, H., Goldbach, R.W., Verduin, B.J.M., 1998. Characterization of the brome mosaic virus movement protein expressed in *E. coli*. Virology 242 (2), 387–394.

Kalinina, N.O., Rakitina, D.A., Yelina, N.E., Zamyatnin Jr., A.A., Stroganova, T.A., Klinov, D.V., Prokhorov, V.V., Ustinova, S.V., Chernov, B.K., Schiemann, J., Solovyev, A.G., Morozov, S.Y., 2001. RNA-binding properties of the 63 kDa protein encoded by the triple gene block of poa semilatent hordeivirus. J. Gen. Virol. 82 (10), 2569–2578.

Kaplan, I.B., Zhang, L., Palukaitis, P., 1998. Characterization of cucumber mosaic virus V. Cell to cell movement requires capsid protein but not virions. Virology 246 (2), 221–231.

Kasteel, D., Wellink, J., Verver, J., van Lent, J., Goldbach, R., van Kammen, A., 1993. The involvement of cowpea mosaic virus M RNA-encoded protein in tubule formation. J. Gen. Virol. 74 (8), 1721–1724.

Kasteel, D.T.J., van der Well, N.N., Jansen, K.A.J., Goldbach, R.W., van Lent, J.W.M., 1997. Tubule-forming capacity of the movement proteins of alfalfa mosaic virus and brome mosaic virus. J. Gen. Virol. 78 (8), 2089–2093.

Kim, S.H., Kalinina, N.O., Andreev, I., Ryabov, E.V., Fitzgerald, A.G., Taliansky, M.E., Palukaitis, P., 2004. The C-terminal 33 amino acids of the cucumber mosaic virus 3a protein affect virus movement, RNA binding and inhibition of infection and translation. J. Gen. Virol. 85 (1), 221–230.

Lazarowitz, S.G., Beachy, R.N., 1999. Viral movement proteins as probes for intracellular and intercellular trafficking in plants. Plant Cell 11 (4), 535–548.

Li, Q.B., Palukaitis, P., 1996. Comparison of the nucleic acid- and NTP-binding properties of the movement protein of cucumber mosaic cucumovirus and tobacco mosaic tobamovirus. Virology 216 (1), 71–79.

Loesch-Fries, L.S., Halk, E.L., Nelson, S.E., Krahn, K.J., 1985. Human leukocyte interferon does not inhibit alfalfa mosaic virus in protoplasts or tobacco tissue. Virology 143 (2), 626–629.

Lucas, W.J., 1995. Plasmodesmata: intercellular channels for macromolecular transport in plants. Curr. Opin. Cell Biol. 7 (5), 673–680.

Marcos, J.F., Villar, M., Pérez-Payá, E., Pallás, V., 1999. In vitro detection, RNA-binding properties and characterization of the RNA-binding domain of the p7 putative movement protein from carnation mottle carmovirus (CarMV). Virology 255 (2), 354–365.

Mc Lean, B.G., Zupan, J., Zambryski, P.C., 1995. Tobacco mosaic virus movement protein associates with the cytoskeleton in tobacco cells. Plant Cell 7 (12), 2101–2114.

Melcher, U., 2000. The 30K superfamily of viral movement proteins. J. Gen. Virol. 81 (1), 257–266.

Mushegian, A.R., Koonin, E.V., 1993. Cell-to-cell movement of plant viruses: insights from amino acid sequence comparisons of movement proteins and from analogies with cellular transport systems. Arch. Virol. 133 (3–4), 239–257.

Pallás, V., Más, P., Sánchez-Navarro, J.A., 1998. Detection of plant RNA viruses by non-isotopic dot–blot hybridization. In: Foster, G., Taylor, S. (Eds.), Plant Virus Protocols: From Virus Isolation to Transgenic Resistance. Humana Press, Totowa, pp. 461–468.

Perbal, M.C., Thomas, C.L, Maule, A.J., 1993. Cauliflower mosaic virus gene I product (P1) forms tubular structures which extend from the surface of infected protoplasts. Virology 195 (1), 281–285.

Rao, A.L.N., 1997. Molecular studies of bromovirus capsid protein: III. Analysis of cell to cell movement competence of coat protein defective variants of cowpea chlorotic mottle virus. Virology 232 (2), 385–395.

Sanchez-Navarro, J.A., Bol, J.F., 2001. Role of the Alfalfa mosaic virus movement protein and coat protein in virus transport. Mol. Plant-Microb. Interact. 14 (9), 1051–1062.

Sanchez-Navarro, J.A., Pallás, V., 1994. Nucleotide sequence of apple mosaic ilarvirus RNA 4. J. Gen. Virol. 75 (6), 1441–1445.

Sanchez-Navarro, J.A., Pallás, V., 1997. Phylogenetical relationships in the ilarviruses: nucleotide sequence of prunus necrotic ringspot RNA 3. Arch. Virol. 142 (4), 749–763.

Sanchez-Navarro, J.A., Reusken, C.B., Bol, J.F., Pallás, V., 1997. Replication of alfalfa mosaic virus RNA 3 with movement and coat protein genes replaced by corresponding genes of Prunus necrotic ringspot Ilarvirus. J. Gen. Virol. 78 (12), 3171–3176.

Sanchez-Navarro, J., Miglino, R., Ragozzino, A., Bol, J.F., 2001. Engineering of alfalfa mosaic virus RNA 3 into an expression vector. Arch. Virol. 146 (5), 923–939.

Schoumacher, F., Gagey, M.J., Maira, M., Stussi-Garaud, C., Godefroy-Colburn, T., 1992. Binding of RNA by the alfalfa mosaic virus movement protein is biphasic. Febs. Lett. 308 (3), 231–234.

Schoumacher, F., Giovane, C., Maira, M., Poirson, A., Godefroy-Colburn, T., Berna, A., 1994. Mapping of the RNA-binding domain of the alfalfa mosaic virus movement protein. J. Gen. Virol. 75 (11), 3199–3202.

Schmitz, I., Rao, A.L.N., 1998. Deletions in the conserve amino-terminal arm of cucumber mosaic virus coat protein disrupt virion assembly but do not abolish infectivity and cell to cell movement. Virology 248 (2), 323–331.

Sreerama, N., Woody, R.W., 2000. Estimation of protein secondary structure from circular dichroism spectra: comparison of CONTIN, SELCON, and CDSSTR methods with an expanded reference set. Anal. Biochem. 287, 252–260.

Tan, R., Frankel, A.D., 1995. Structural variety of arginine-rich RNA-binding peptides. Proc. Natl. Acad. Sci. U.S.A. 92, 5282–5286.

Takeda, A., Kaido, M., Okuno, T., Mise, K., 2004. The C terminus of the movement protein of Brome mosaic virus controls the requirement for coat protein in cell-to-cell movement and plays a role in long-distance movement. J. Gen. Virol. 85 (6), 1751–1761.

Taschner, P.E., Van der Kuyl, A.C., Neeleman, L., Bol, J.F., 1991. Replication of an incomplete alfalfa mosaic virus genome in plants transformed with viral replicase genes. Virology 181 (2), 445–450.

Tenllado, F., Bol, J.F., 2000. Genetic dissection of the multiple functions of alfalfa mosaic virus coat protein in viral RNA replication, encapsidation, and movement. Virology 268, 29–40.

Thomas, C.L., Maule, A.J., 1995. Identification of structural domains within the cauliflower mosaic-virus movement protein by scanning deletion mutagenesis and epitope tagging. Plant Cell 7 (5), 561–572.

van der Wel, N.N., Goldbach, R.W., van Lent, J.W., 1998. The movement protein and coat protein of alfalfa mosaic virus accumulate in structurally modified plasmodesmata. Virology 244 (2), 322–329.

van Dun, C.M., van Vloten-Doting, L., Bol, J.F., 1988. Expression of alfalfa mosaic virus cDNA1 and 2 in transgenic tobacco plants. Virology 163 (2), 572–578.

van Lent, J., Wellink, J., Goldbach, R., 1990. Evidence for the involvement of the 58K and 48K proteins in the intercellular movement of cowpea mosaic-virus. J. Gen. Virol. 71, 219–223.

Vaquero, C., Liao, Y.-C., Nähring, J., Fisher, R., 1997. Mapping of the RNA-binding domain of the cucumber mosaic virus movement protein. J. Gen. Virol. 78 (8), 2095–2099.

Vilar, M., Esteve, V., Pallás, V., Marcos, J.F., Pérez-Payá, E., 2001. Structural properties of Carnation mottle virus p7 movement protein and its RNA-binding domain. J. Biol. Chem. 276 (21), 18122–18129.

Vilar M., Saurí A., Marcos, F.J., Mingarro I., Pérez-Payá, E., in press. Transient structural ordering of the RNA-binding domain of carnation mottle virus p7 movement protein modulates nucleic acid binding. Chem. Bio. Chem.

Vlot, A.C., Neeleman, L., Linthorst, H.J., Bol, J.F., 2001. Role of the 3′-untranslated regions of alfalfa mosaic virus RNAs in the formation of a transiently expressed replicase in plants and in the assembly of virions. J. Virol. 75 (14), 6440–6449.

Waigmann, E., Ueki, S., Trutnyeva, K., Citovsky, V., 2004. The ins and outs of non-destructive cell-to-cell and systemic movement of plant viruses. Crit. Rev. Plant Sci. 23 (3), 195–250.

Wobbe, K.K., Akgoz, M., Dempsey, D.A., Klessig, D.F., 1998. A single amino acid change in turnip crinkle virus movement protein p8 affects RNA binding and virulence on *Arabidopsis thaliana*. J. Virol. 72 (7), 6247–6250.

Wolf, S., Deom, C.M., Beachy, R.N., Lucas, W.J., 1989. Movement protein of tobacco mosaic-virus modifies plasmodesmatal size exclusion limit. Science 246 (4928), 377–379.

Zheng, H.Q., Wang, G.L., Zhang, L., 1997. Alfalfa mosaic virus movement protein induces tubules in plant protoplasts. Mol. Plant-Microb. Interact. 10 (8), 1010–1014.